Desalination and Water Treatment
www.deswater.com

doi: 10.1080/19443994.2016.1152647

57 (2016) 24615–24625
November

Taylor & Francis
Taylor & Francis Group

Theoretical and experimental investigation of boron rejection by forward osmosis membrane

Yong-Jun Choi[a], Sangho Lee[a,*], Jaewuk Koo[a,b], Tae-Mun Hwang[b]

[a]*School of Civil and Environmental Engineering, Kookmin University, Jeongneung-Dong, Seongbuk-Gu, Seoul 136-702, Republic of Korea, Tel. +82 2 910 5060; email: choiyj1041@gmail.com (Y.-J. Choi), Tel. +82 2 910 4529; Fax: +82 2 910 4939; email: sanghlee@kookmin.ac.kr (S. Lee), Tel. +82 31 910 0755; email: koojaewuk@naver.com (J. Koo)*
[b]*Department of Construction Environmental Research, Korea Institute of Construction Technology, 2311 Daehwa-Dong, Ilsan-Gu, Goyang-Si, Gyeonggi-Do 411–712, South Korea, Tel. +82 31 910 0741; email: taemun@kict.re.kr (T.-M. Hwang)*

Received 23 October 2015; Accepted 8 January 2016

ABSTRACT

This study focused on the investigation of the boron rejection from model solutions using a forward osmosis (FO) membrane. A laboratory-scale plate-and-frame membrane module and stirred cell device were used for the experiments. The boron rejection were examined in both reverse osmosis and FO operating modes. A theoretical model based on the film theory was applied for the analysis of boron rejection. Experimental results indicated that the boron rejection by FO membranes was improved by raising pH, suggesting that the removal of boron is done either by charge repulsion or by size exclusion. FO treatment of feedwater containing a high proportion of boric acid led to relatively high concentration of boron in the permeate water. This implies that FO membrane may require another process to attain sufficient rejection to boron. The model calculation was also compared with the experimental data for better understanding of boron rejection in FO membrane systems.

Keywords: Forward osmosis; Boron; Seawater desalination; Rejection; Modeling

---

1. Introduction

Desalination of seawater and brackish water is becoming increasingly important due to water scarcity resulting from pollution and the growth of population. One of the promising approaches to seawater desalination is the application of forward osmosis (FO) membrane [1,2]. FO uses a concentrated draw solution to generate high osmotic pressure, which pulls water across a semi-permeable membrane from the feed solution. The draw solute is then separated from the diluted draw solution to recycle the solute, as well as to produce clean product water [1]. Since FO does not require high pressure for separation, it has potential to allow lower energy consumption to produce water than reverse osmosis (RO). Therefore FO, a potential alternative to conventional membrane processes, has been considered a novel technology for seawater desalination [2].

However, there are challenges that have to be overcome to apply FO process for seawater desalination.

---

*Corresponding author.

Presented at 2015 Academic Workshop for Desalination Technology held in the Institute for Far Eastern Studies Seoul, Korea, 23 October 2015

One of them is the removal of boron from seawater. Boron is an essential micronutrient for plants and animals [3], and also a useful component for numerous commercial activities, including glass industry and semiconductor manufacture [4]. However, excess boron can cause toxic effects in both plants and animals [3–7]. For example, crops such as avocado and most citrus types are sensitive to boron at the concentration range 0.5–0.75 mg/L [8]. Although the World Health Organization had recently updated up the guidelines for boron concentration in drinking water from 0.5 to 2.4 mg/l [9], the demand to maintain a low level of boron concentration (0.3–0.8 mg/L) in desalinated waters will remain unchanged [10].

Boron exists in the seawater at an average concentration of 4–6 mg/L [11,12]. In seawater, dissolved boron is present as boric acid, $B(OH)_3$ and borate ion, $B(OH)_4^-$, depending on the pH and concentration of boron [13]. The distribution of two components, boric acid and borate ion, depends on the dissociation constant of boric acid (pK_a), which is a function of temperature, pressure, pH, and ionic strength. In typical seawater conditions, the dissociation constant is approximately 8.7. Thus, boric acid is the major form of boron in natural seawater (pH of ~8) [13]. Since boric acid is an uncharged compound, its removal by RO membrane is difficult, leading to relatively high boron concentration in the treated water [14].

Considering the mechanisms of boron rejection by RO and FO membranes [8,13], it is likely that the removal of boron by FO is also difficult. This implies that boron rejection should be considered in the design and operation of the FO process for seawater desalination. Accordingly, this study aims at the investigation of the boron rejection from model solutions using an FO membrane. The effect of solution pH and operation mode on boron rejection by FO was considered using a laboratory-scale experimental system. Moreover, theoretical analysis was carried out for better understanding of boron rejection in FO process.

2. Theory

A theoretical model was applied to calculate the transport coefficients of water, salt, and boron through an FO membrane operated in RO and FO modes. According to the solution-diffusion model, water flux (J_w), salt flux (J_s) and boron flux (J_{s_B}) equations for RO operation mode are given by [15]:

$$J_w = L_v(\Delta P - \Delta\pi_{C_m}) \tag{1}$$

$$J_s = L_s(C_m - C_p) \tag{2}$$

$$J_{s\_B} = L_{s\_B}(C_{m\_B} - C_{p\_B}) \tag{3}$$

where L_v is the water transport coefficient, L_s is the salt transport coefficient, L_{s_B} is the boron transport coefficient, C_m is the salt concentration on the membrane surface, C_{m_B} is the boron concentration on the membrane surface, C_p is the salt concentration at the permeate side, C_{p_B} is the boron concentration at the permeate side, $\Delta\pi_{C_m}$ is the osmotic pressure at the salt concentration of C_m and ΔP is the trans-membrane pressure.

Here, C_m is calculated according to the film theory to interpret the concentration polarization, and the salt concentration profile on the surface can be calculated according to the following equation [15].

$$\frac{C_m - C_p}{C_b - C_p} = e^{\frac{J_w}{k}} \tag{4}$$

where k is the mass transfer coefficient for the back diffusion of the solute from the membrane to the bulk solution on the high-pressure side of the membrane.

In a stirred cell, the growth of the concentration boundary layer is limited by stirring according to the mass transfer coefficient, using the following equation [16]:

$$k = 0.5510\left(\frac{ud_h}{v}\right)^{0.4}\left(\frac{v}{D}\right)^{0.17}\left(\frac{C_b}{\rho}\right)^{-0.77}\left(\frac{D}{d_h}\right)^{-0.77} \tag{5}$$

where u is the crossflow velocity, d_h is the hydraulic diameter, v is the kinematic viscosity, ρ is the solution density.

The boron concentration on the membrane surface, C_{m_B} is calculated same as C_m.

For FO operation mode, the water flux (J_w), solute flux (J_s), and boron flux (J_{sb}) equations can be defined as follows [17]:

$$J_w = L_v\left(\pi_{D,b}\exp\left(-\frac{J_w}{k_D}\right) - \pi_{F,b}\exp\left(\frac{J_w}{k_F}\right)\right) \tag{6}$$

$$J_s = L_s\left(C_{D,b}\exp\left(-\frac{J_w}{k_D}\right) - C_{F,b}\exp\left(\frac{J_w}{k_F}\right)\right) \tag{7}$$

$$J_{s\_B} = L_{s\_B}\left(C_{F,b\_B}\exp\left(\frac{J_w}{k_F}\right) - C_{D,b\_B}\exp\left(-\frac{J_w}{k_D}\right)\right) \tag{8}$$

where $\pi_{D,b}$ is the osmotic pressure on the draw bulk solution side, $\pi_{F,b}$ is the osmotic pressure on the feed bulk side, $C_{D,b}$ and $C_{F,b}$ are the salt concentrations of the draw bulk solution and the feed bulk solution, respectively, C_{D,b_B} and C_{F,b_B} are the boron concentrations of the draw bulk solution and the feed bulk solution, respectively, k_F is the mass transfer coefficient for external concentration polarization, k_D is the mass transfer coefficient for internal concentration polarization.

Base on the mass transfer correlations, k_F and k_D are given as [15]:

$$k_F = 1.85 \frac{D}{d_h^{0.65} L^{0.33}} (R_e S_c)^{0.33} \tag{9}$$

$$k_D = \frac{D\varepsilon}{\tau l} \tag{10}$$

where D is the diffusion coefficient, d_h is the hydraulic diameter, R_e is the Reynolds number, S_c is the Schmidt number, ε is the porosity of support layer, l is the thickness of support layer, and τ is the tortuosity of support layer.

3. Materials and methods

3.1. Materials

Commercially available flat sheet FO membranes manufactured by Hydration Technologies (Albany, OR), was used in this study. This membrane is known to be made of cellulose triacetate. Reagent-grade boric acid, sodium chloride, hydrochloric acid, and caustic soda from Merck (Damsdalt, Germany), were used in the experiments. Dried boric acid and sodium chloride were dissolved directly into DI water according to respective experimental concentration while 0.1 M hydrochloric acid and 0.1 M caustic soda were prepared for pH adjustment during the experiments.

3.2. Setup

The boron rejection experiments in RO operation mode were performed in batch mode using a stirred cell as shown in Fig. 1. The stirred cell was made of 316L stainless steel. The diameter of the stirred cell was 49 mm and the working volume was 300 ml. A magnetic stirrer coated with Teflon to improve chemical stability was positioned just above the membrane. The working pressure was controlled by a high pressure nitrogen cylinder and by a gas pressure regulator. A feed solution was prepared by adding boric acid into 50 mL of DI water to make 5 mg/L of boron. Then, required amounts of NaCl (32,000 mg/L) were added and pH adjusted. The experiments were carried out under the following operating conditions: the feed pressure, 32 bar; stirring speed, 100 rpm; recovery (the ratio of total permeate volume to initial feed volume), 40%. The temperature of the feed solution was adjusted to 25 ± 1℃. The permeate flux was consecutively measured using the balance (Ohaus, UK) that was connected to the computer.

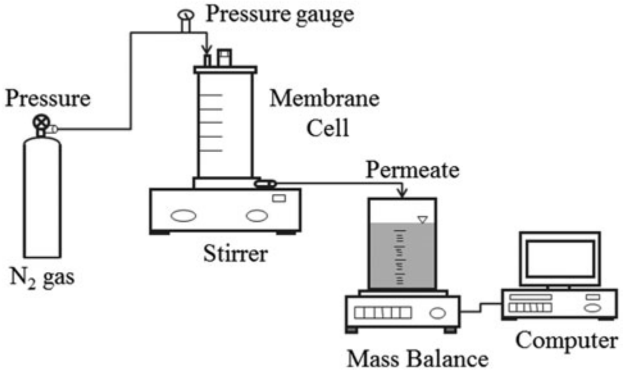

Fig. 1. Schematic diagram of the stirred cell device.

The FO filtration system shown in Fig. 2 was used to measure boron rejection. A plate-and-frame membrane module was used for the tests. Counter-current flow is used to reduce strain on the suspended membrane. The draw and feed solution volume flow rate were 1.0 L/min. The channel has dimensions of 8 cm length, 7 cm width, and 0.3 cm height, providing an effective membrane area of 5.6 cm^2. The draw solution is flowing on the support layer and the feed solution on the active layer. An electronic balance connected to a personal computer was used to measure the water flux. 1.0 L of 4 M, NaCl solution was used for draw solution, and 0.4 L of 32,000 mg/L, NaCl solution was used for feedwater. The temperature of draw and feed solution was maintained to be constant at 25 ± 1℃ by a temperature control unit.

3.3. Sample analysis

The boron rejection, permeate boron concentration, and flux were expressed in terms of concentration factor (F_c). The concentration factor, defined as a ratio of the feed volume to concentrate volume, indicates the extent of concentration:

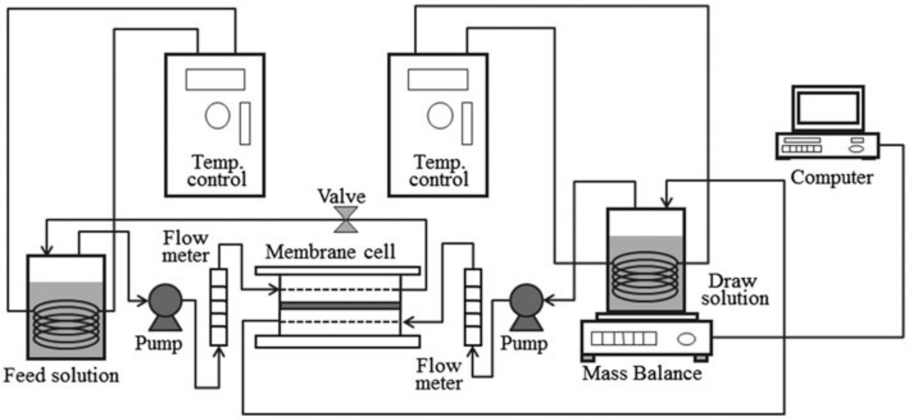

Fig. 2. Diagram of the FO membrane filtration system.

$$F_c = \frac{V_F}{V_C} = \frac{V_F}{V_F - V_P} \tag{11}$$

where V_F is the feed volume, V_C is the concentrate volume, and V_P is the permeate volume.

Boron was analyzed by ion-coupled plasma optical emission spectrometry (ICP-OES) model Optima 5300DV of PerkinElmer (Waltham, MA, USA). Other parameters such as pH and temperature were measured by potable meters (Thermo-Scientific, 550A from USA).

4. Results and discussion

4.1. Basic properties of the FO membrane

In order to evaluate the basic properties of the FO membrane, pure water permeability and NaCl rejection were measured in RO operation mode using the batch-stirred cell. Pure water permeability test was carried out at the feed pressure as to range from 5 to 40 bar. NaCl rejection tests were carried out under the following operating conditions: the feed pressure, 32 bar; stirring speed, 100 rpm; feed concentration, 32,000 mg/L. The water permeability coefficient, L_v, and salt permeability coefficient, L_s obtained were 3.52×10^{-12} m/s Pa and 6.07×10^{-8} m/s, respectively (Fig. 3).

4.2. Boron rejection in RO operation mode

Fig. 4 shows the comparison of boron rejection and water flux at different pH conditions in RO operation mode. Except for pH conditions, all other experimental conditions including feed pressure, feed temperature, feed salt concentration, boron concentration, and

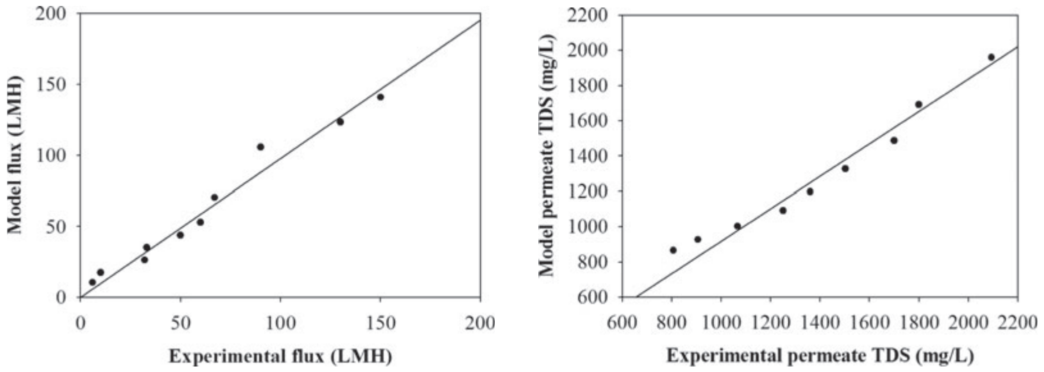

(a) (b)

Fig. 3. Comparison of experimental data and model data to find water permeability coefficient and salt permeability coefficient of the FO membrane: (a) Flux and (b) Permeate TDS (mg/L).

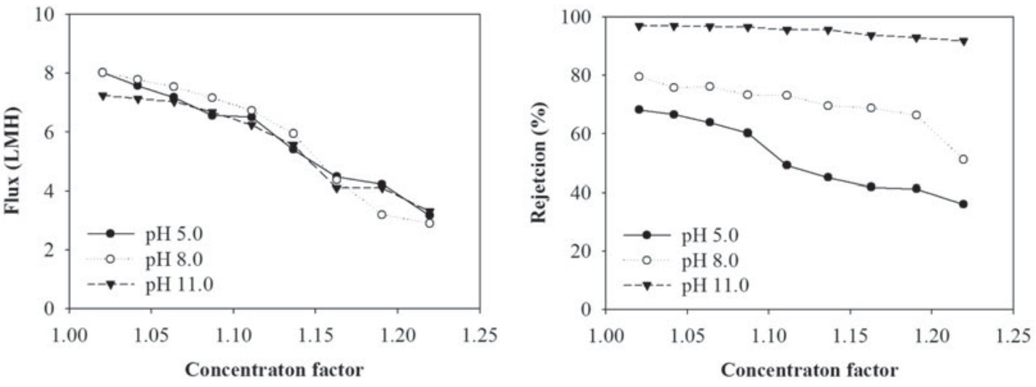

(a) (b)

Fig. 4. Comparison of boron rejection and water flux at different pH conditions in RO operation mode: (a) Flux and (b) Boron rejection.

stirring speed were constant. In other words, only the impact of pH on boron rejection was determined. RO operation mode tests were carried out under the following operating conditions: pH 5.0/8.0/11.0; the feed pressure, 32 bar; stirring speed, 100 rpm; feed concentration, 32,000 mg/L; boron concentration, 5.0 mg/L. The feed pressure was determined 32.0 bar to obtain the same initial flux as that in FO operation mode.

The permeate flux was constant regardless of pH change, but the permeate flux decreased as the concentration factor increased shown as Fig. 4. When the concentration factor was reached to 1.22, the flux decreased to approximately 3.0 LMH compared with the initial flux, 8.0 LMH. This was due to an increase in the osmotic pressure, as the concentration of the feed solution was enriched according to the concentration factor. Boron rejection increased as the pH increased but boron rejection decreased rapidly as concentration factor increased because flux rapidly decreased due to increasing of osmotic pressure. The boron rejection was very low at pH 5.0 and 8.0 where rejection efficiencies were around 36–68% and 51–80%, respectively. In RO operation mode, the FO membrane did not produce drinking water that satisfies the low boron concentration (0.3–0.8 mg/L) under pH 8.0. But at pH 11.0, the rejection increases up to 93–98% to achieve low boron concentration under 0.5 mg/L, due to the increased proportion of borate ions as the pH rises. The results of high boron rejection at high pH condition suggest that the major species of boron are borate ions which have negative charge and thus electrostatic repulsion between the ions and membrane surface become more dominant at high pH condition.

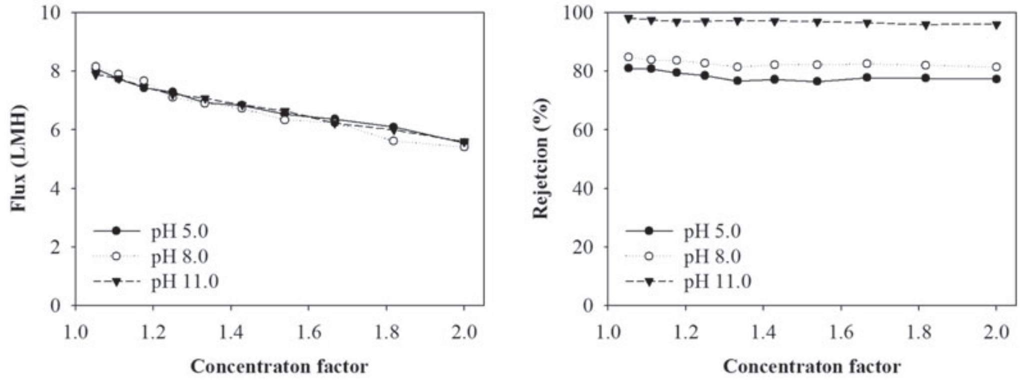

(a) (b)

Fig. 5. Comparison of boron rejections and water flux at different pH conditions in FO operation mode: (a) Flux and (b) Boron rejection.

4.3. Boron rejection tests in FO operation mode

Fig. 5 shows the comparison of boron rejection and water flux at different pH conditions in FO operation mode. FO operation mode tests were carried out under the following operating conditions: draw solution concentration, NaCl 4 M, feed salt concentration, 32,000 mg/L; feed boron concentration, 5.0 mg/L; cross flow, 1 L/min.

The filtration characteristics in FO operation mode are similar to those in RO mode. As the concentration factor increased, the permeate flux gradually decreased because of decreased driving force (osmotic pressure difference between feed and draw solution sides). The permeate flux was low even at high draw solution concentration, 4 M ranged from 7.9 to 8.2 LMH due to internal concentration polarization. The boron rejection characteristics in FO mode are different to those in RO mode. The boron rejection was found to range from 77 to 81% and from 81 to 85% at pH 5.0 and 8.0, respectively. The boron rejection in FO mode is much higher than that in RO mode under pH 8.0. In FO operation mode, FO membrane also did not produce drinking water that satisfies the low boron concentration (0.3–0.8 mg/L) under pH 8.0. But at pH 11.0, the rejection increases up to 96–98% to achieve low boron concentration due to the increased proportion of borate ions as the pH rises.

4.4. Model fit

For each pH condition and operation mode, the model calculation was performed to find the parameters that minimize the difference between model predictions and experimental results under different concentration factor. Thus, the R^2 value was calculated:

$$R_1^2 = \sum_{i=1}^{N} (J_{v,i\_m} - J_{v,i\_e})^2 / J_{v,i\_m}^2$$

$$R_2^2 = \sum_{i=1}^{N} (C_{p,i\_m} - C_{v,i\_e})^2 / C_{p,i\_m}^2$$

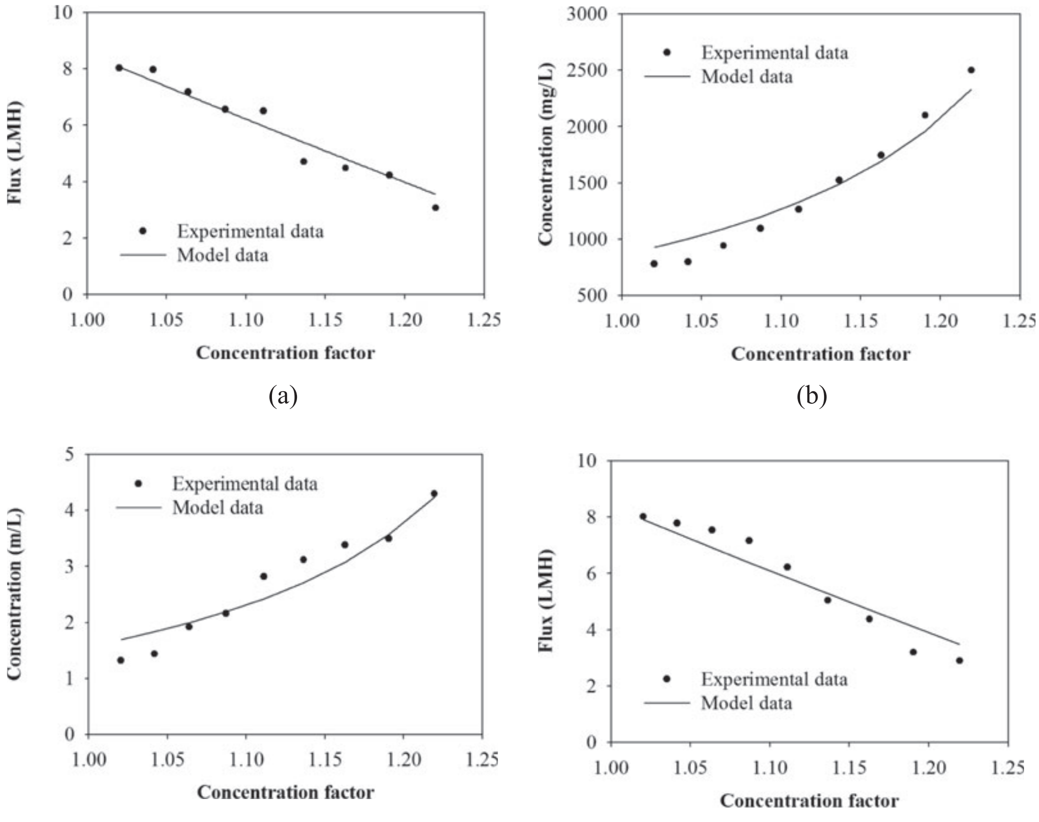

(a) (b)

(c) (d)

Fig. 6. Model fit base on the test results in RO operation mode: (a) flux at pH 5.0, (b) permeate conc. at pH 5.0, (c) boron conc. at pH 5.0, (d) flux at pH 8.0, (e) permeate conc. at pH 8.0, (f) boron conc. at pH 8.0, (g) flux at pH 11.0 (h) permeate conc. at pH 11.0, and (i) boron conc. at pH 11.0.

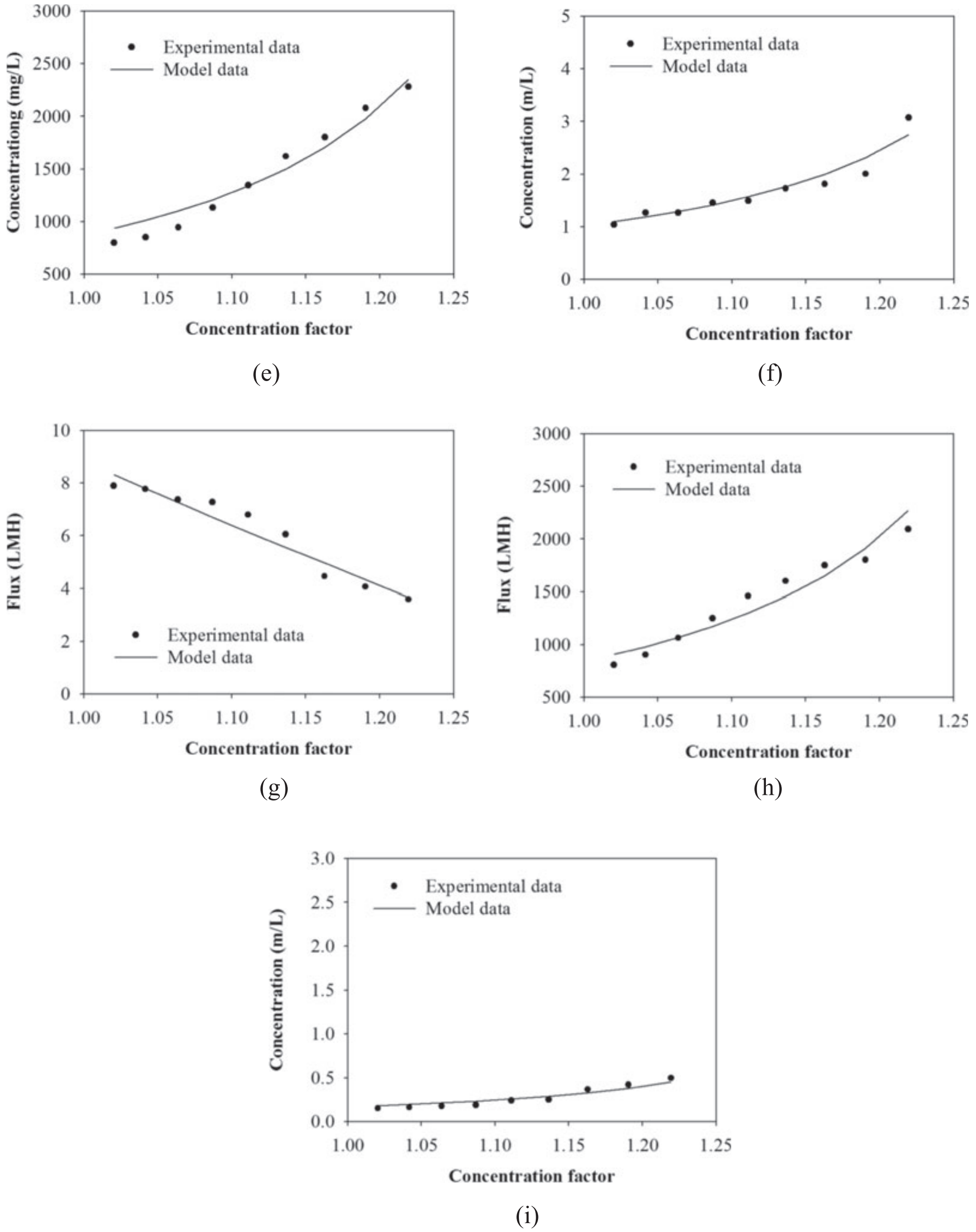

(e) (f)

(g) (h)

(i)

Fig. 6. (*Continued*).

$$R_3^2 = \sum_{i=1}^{N} (C_{pb,i\_m} - C_{pb,i\_e})^2 / C_{pb,i\_m}^2$$

where N is the total number of experimental data, J_{v,i_m} is the ith value for calculated flux, J_{v,i_e} is the ith value for the experimental flux, C_{p,i_m} is the ith value for calculated TDS, C_{p,i_e} is the ith value for the experimental TDS, C_{pb,i_m} is the ith value for calculated boron concentration, and C_{pb,i_e} is the ith value for the experimental boron concentration.

Fig. 6 shows the model fit of the test results of RO operation mode and the analysis results of the solution-diffusion model, while considering the concentration polarization. The model calculation was performed to find the parameters (L_v, L_s, L_{s_B}) that will minimize the difference between the model predictions and the experiment results under different

Table 1
Comparison of parameters in RO operation mode for each pH

pH	L_v (m^2 s/kg)	L_s (m/s)	L_{sb} (m/s)	R^2 ($L_v/L_s/L_{sb}$)
5.0	3.52×10^{-12}	6.07×10^{-8}	7.15×10^{-7}	0.17/0.22/0.35
8.0	3.45×10^{-12}	6.01×10^{-8}	4.53×10^{-7}	0.22/0.19/0.17
11.0	3.60×10^{-12}	6.10×10^{-8}	0.78×10^{-7}	0.14/0.20/0.28

experiment conditions using the residual constant R^2. It is evident from the model fit that the test results and the model data are relatively matched well. As shown in Table 1, the water, salt, and boron transport parameters were calculated, respectively.

There were few changes of L_v and L_s regardless of pH change, but the L_{s_B} decreased as the pH increased. Especially at pH 11.0, L_{s_B} rapidly decreased.

Fig. 7 shows the results of model fit to the test data in FO operation mode. The model matches the experimental data very well. The internal concentration polarization coefficient was calculated as 1.30×10^{-6} m/s. As shown in Table 2, the solvent transport parameter and the solute transport parameter were calculated. There were few changes of L_v and L_s regardless of pH change but the L_{s_B} decreased as the pH increased same as RO operation mode.

The model fit results showed that the boron transport coefficient in FO operation mode is about 18% lower than that in the RO operation mode under pH 8.0 for the same membrane. This means that the boron rejection in FO operation mode is higher than that in RO operation mode under pH 8.0. It has been reported that the boron rejection in FO operation mode was mainly attributed to reverse salt diffusion

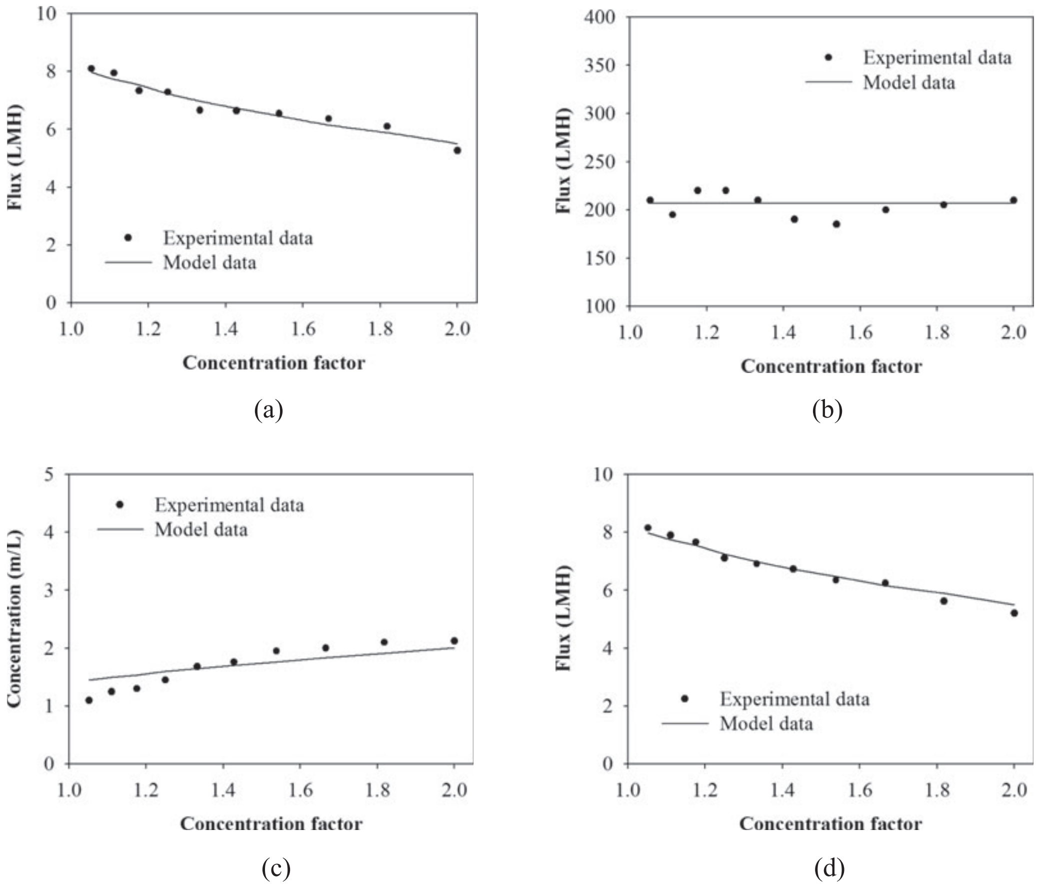

(a) (b)

(c) (d)

Fig. 7. Model fit base on the test results in FO operation mode: (a) flux at pH 5.0, (b) permeate conc. at pH 5.0, (c) boron conc. at pH 5.0, (d) flux at pH 8.0, (e) permeate conc. at pH 8.0, (f) boron conc. at pH 8.0, (g) flux at pH 11.0 (h) permeate conc. at pH 11.0, and (i) boron conc. at pH 11.0.

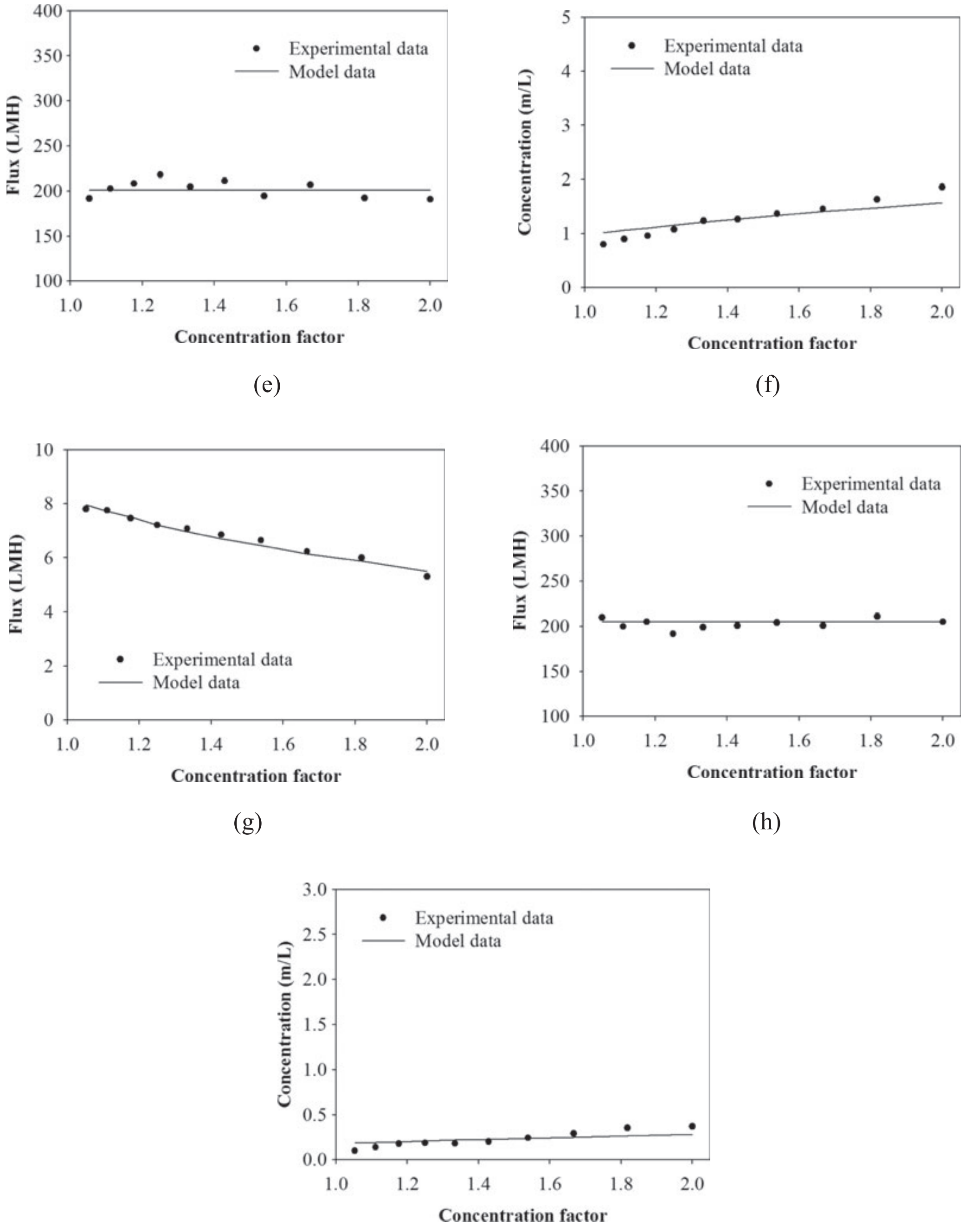

(e) (f)

(g) (h)

(i)

Fig. 7. (*Continued*).

Table 2
Comparison of parameters in FO operation mode for each pH

pH	L_v (m^2 s/kg)	L_s (m/s)	L_{sb} (m/s)	R^2 ($L_v/L_s/L_{sb}$)
5.0	3.52×10^{-12}	6.07×10^{-8}	5.70×10^{-7}	0.08/0.10/0.11
8.0	3.50×10^{-12}	6.07×10^{-8}	3.8×10^{-7}	0.12/0.10/0.11
11.0	3.48×10^{-12}	6.00×10^{-8}	0.73×10^{-7}	0.10/0.12/0.10

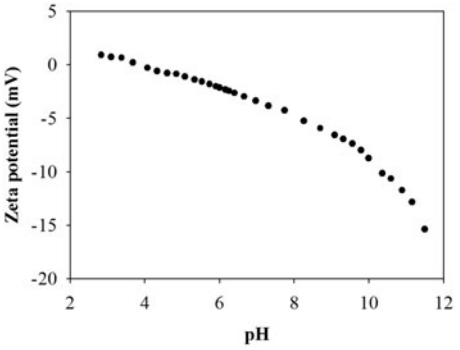

Fig. 8. Zeta potentials of the FO membrane a function of solution pH.

[18]. However, the value of L_{s_B} in FO mode is almost identical to that in RO mode at pH 11.0 since the boron is removed by size exclusion and charge repulsion at high pH condition.

In the FO operation mode, permeate salt concentration was calculated by dividing the salt flux by the water flux (J_s/J_v). The permeate salt concentration is constant regardless of concentration factor since the decrease ratio of salt flux and water flux was same in accordance with increasing concentration factor.

4.5. Zeta potential of FO membrane

Zeta potential of the FO membrane was measured under different pH conditions using a streaming potential analyzer (SurPASS, AntonPaar GmbH, Graz, Austria). A background electrolyte solution of 10 mM KCl was used, and solution pH was adjusted to be within the range of pH 3.0–11.5 with proper addition of 0.1 M of HCl or NaOH. Measurements were conducted at a temperature of 24–25˚C and zeta potential was calculated from the measured streaming potential using the Helmholtz–Smoluchowski equation with the Fair brother and Mastin substitution [19]. Zeta potential of the FO membrane decreased rapidly with increasing pH shown as Fig. 8. This means that the boron rejection by the FO membrane using this study has been improved through raised pH since the force of repulsion between boron and membrane increased with increasing pH.

5. Conclusions

In this study, theoretical and experimental analysis of boron rejection by FO membranes was investigated. The following conclusions were withdrawn:

(1) Experiments were conducted to investigate the impacts of pH and operation mode on boron rejection in RO and FO operation modes. In both cases, the boron rejection increases with increasing the pH of feed solution. However, the higher boron rejection in FO compared to RO was observed under acidic (pH 5) and neutral conditions (pH 8), which is mainly attributed to reverse salt diffusion [8].

(2) At pH 11, the boron rejections in RO and FO operation modes were similar, implying that boron in the form of negatively charged borate ion separated in FO mode is similar to those in RO mode.

(3) Similar to RO, the overall boron rejection by FO is dependent on the boric acid/borate ion ratio. In other words, the FO membrane for feedwater under acidic and neutral pH conditions will lead to relatively high levels of boron in the permeate water.

(4) The application of the solution–diffusion model was found to be effective to understand the transport properties of ions and boron species through the FO membrane.

Acknowledgment

This research was supported by a grant(code 15IFIP-B065893-03) from Industrial Facilities & Infrastructure Research Program funded by Ministry of Land, Infrastructure and Transport of Korean government.

References

[1] J.R. McCutcheon, R.L. McGinnis, M. Elimelech, A novel ammonia–carbon dioxide forward (direct) osmosis desalination process, Desalination 174 (2005) 1–11.

[2] J.R. McCutcheon, R.L. McGinnis, M. Elimelech, Desalination by ammonia–carbon dioxide forward osmosis: Influence of draw and feed solution concentrations on process performance, J. Membr. Sci. 278 (2006) 114–123.

[3] R. Reid, Update on boron toxicity and tolerance in plants, in: F. Xu, H.E. Goldbach, P.H. Brown, R.W. Bell, T. Fujiwara, C.D. Hunt, S. Goldberg, L. Shi (Eds.), Advances in Plant and Animal Boron Nutrition: Proceedings of the 3rd International Symposium on All Aspects of Plant and Animal Boron Nutrition, Springer, Dordrecht, 2007, pp. 83–90.

[4] R.J. Weir, R.S. Fisher, Toxicologic studies on borax and boric-acid, Toxicol. Appl. Pharmacol. 23 (1972) 351–364.

[5] D.A. Roe, D.B. McCormick, R.T. Lin, Effects of riboflavin on boric acid toxicity, J. Pharm. Sci. 61 (1972) 1081–1085.

[6] Toxicology and Carcinogenesis Studies of Boric Acid (CAS No. 10043-35-3) in B6C3F1 Mice (Feed Studies), National Toxicology Program Tech Rep Ser. 1987 October, vol. 324, pp. 1–126.

[7] W.W. Ku, R.E. Chapin, R.F. Moseman, R.E. Brink, K.D. Pierce, K.Y. Adams, Tissue disposition of boron in male Fischer rats, Toxicol. Appl. Pharmacol. 111 (1991) 145–151.

[8] N. Hilal, G.J. Kim, C. Somerfield, Boron removal from saline water: A comprehensive review, Desalination 273(1) (2011) 23–35.

[9] World Health Organization (WHO), Guidelines for Drinking-water Quality, fourth edition, 2011. Available from: <http://www.who.int/water_sanitation_health/publications/2011/dwq_guidelines/en/>.

[10] O. Nir, M. Herzberg, A. Sweity, L. Birnhack, O. Lahav, A novel approach for SWRO desalination plants operation, comprising single pass boron removal and reuse of CO_2 in the post treatment step, Chem. Eng. J. 187 (2012) 275–282.

[11] W.G. Woods, An introduction to boron: History, sources, uses, and chemistry, Environ. Health Perspect. 102(Suppl 7) (1994) 5–11.

[12] H. Koseoglu, N. Kabay, M. Yüksel, S. Sarp, Ö. Arar, M. Kitis, Boron removal from seawater using high rejection SWRO membranes—Impact of pH, feed concentration, pressure, and cross-flow velocity, Desalination 227(1–3) (2008) 253–263.

[13] H. Hyung, J.-H. Kim, A mechanistic study on boron rejection by sea water reverse osmosis membranes, J. Membr. Sci. 286 (2006) 269–278.

[14] M.H. Oo, S.L. Ong, Implication of zeta potential at different salinities on boron removal by RO membranes, J. Membr. Sci. 352 (2010) 1–6.

[15] J.G. Wijmans, R.W. Baker, The solution–diffusion model: A review, J. Membr. Sci. 107 (1995) 1–21.

[16] S. Nicolas, B. Balannec, F. Beline, B. Bariou, Ultrafiltration and reverse osmosis of small non-charged molecules: A comparison study of rejection in a stirred and an unstirred batch cell, J. Membr. Sci. 164 (2000) 141–155.

[17] T.Y. Cath, A.E. Childress, M. Elimelech, Forward osmosis: Principles, applications, and recent developments, J. Membr. Sci. 281 (2006) 70–87.

[18] C. Kim, S. Lee, H.K. Shon, M. Elimelech, H.K. Shon, S.k. Hong, Boron transport in forward osmosis: Measurements, mechanisms, and comparison with reverse osmosis, J. Membr. Sci. 419–420 (2012) 42–48.

[19] M. Elimelech, W.H. Chen, J.J. Waypa, Measuring the zeta (electrokinetic) potential of reverse osmosis membranes by a streaming potential analyzer, Desalination 95 (1994) 269–286.